Lipophilic siRNA Targets Albumin *in Situ* and Promotes Bioavailability, Tumor Penetration, and Carrier-Free Gene Silencing

Samantha M. Sarett[1], Thomas A. Werfel[1], Lee L[1], Meredith A. Jackson[1], Kameron V. Kilchrist[1], Dana Brantley-Sieders[2], Craig L. Duvall[1]
[1]Vanderbilt University, Department of Biomedical Engineering
[2]Vanderbilt University Medical Center, Department of Medicine

Supplementary Information:

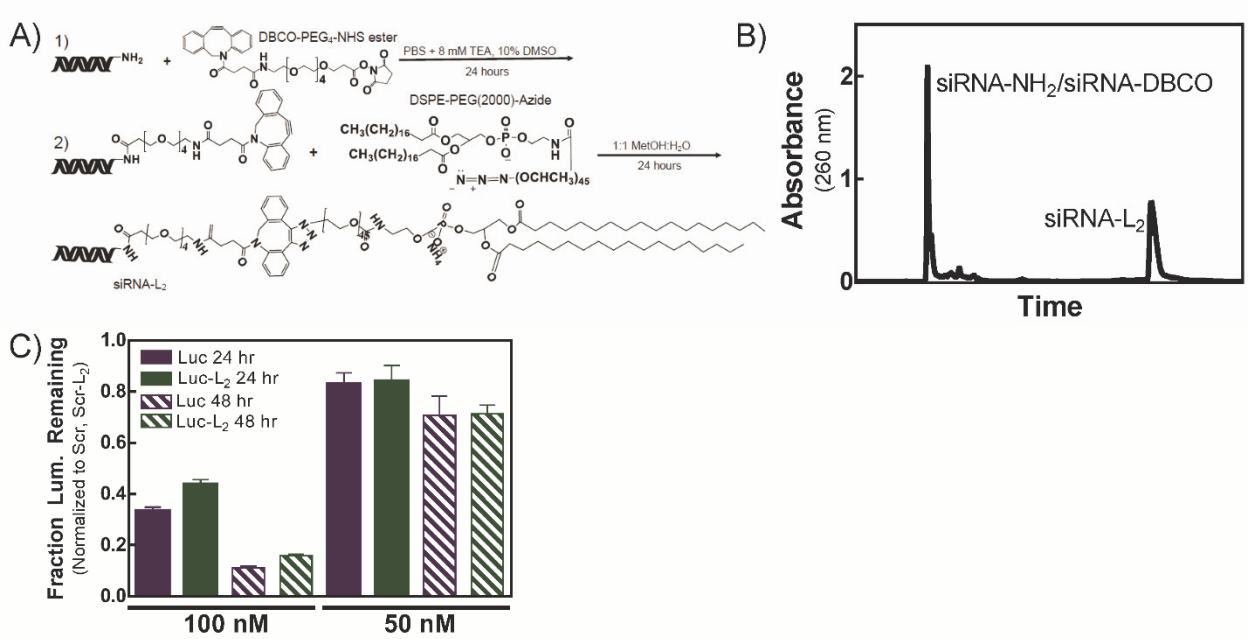

Figure S1. A) Full chemical structures of reactants and final product siRNA-L_2. Synthesis scheme is two-step; 1) siRNA-NH_2 + DBCO-PEG_4-NHS ester, 2) siRNA-DBCO + DSPE-PEG(2000)-azide. B) HPLC purification of siRNA-L_2 conjugate from reactant precursors. C) L_2 conjugation does not impact siRNA silencing efficacy. A comparison of siRNA and siRNA-L_2 silencing from *in vivo* jetPEI at a dose of 100 nM; n of 5, standard error shown.

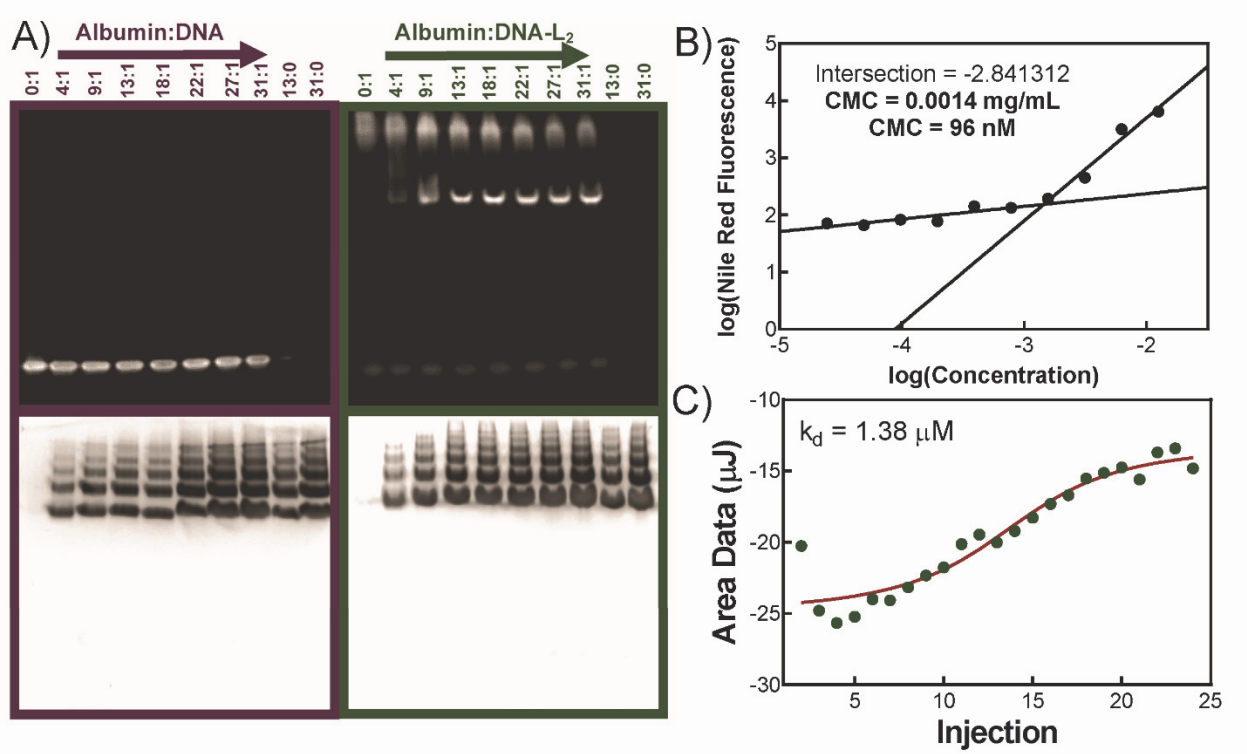

Figure S2. A) Albumin binding of DNA-L_2 as measured by non-denaturing PAGE gel stained for DNA (top) and BSA (bottom). DNA-L_2 migrates as a micellar population alone and co-migrates with albumin. Unmodified siRNA does not migrate with albumin. Molar ratio of albumin:oligo is indicated. B) Critical micelle concentration of siRNA-L_2 as determined via Nile Red assay. C) Isothermal calorimetry (ITC) shows exothermic binding of siRNA-L_2 to bovine serum albumin (BSA) with a dissociation constant of 1.38 μM.

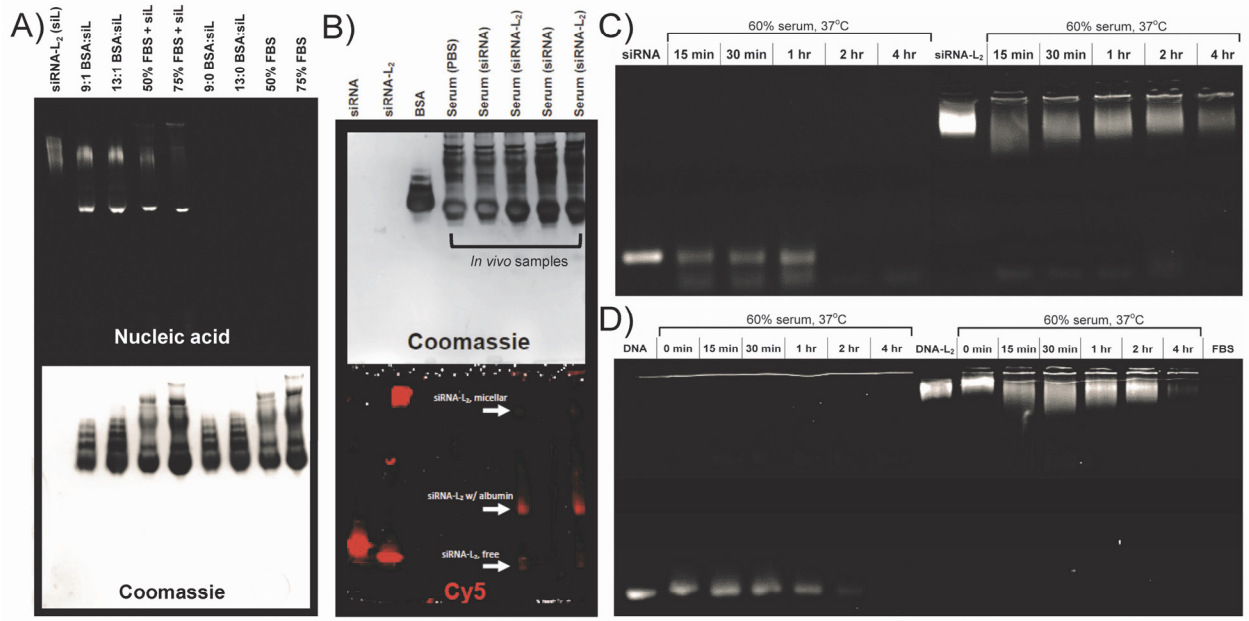

Figure S3. A) Evaluation of association of siRNA/siRNA-L_2 with BSA or serum albumin in complete FBS by PAGE gel retardation assay. siRNA-L_2 alone (far right) migrates as a micellar population. Bound siRNA-L_2 migrates in the same location when mixed with BSA or FBS, suggesting that siRNA-L_2 is associating with the albumin component of FBS. Also shown are protein controls of BSA (middle, left) and FBS (far left). B) siRNA-L_2 associates with albumin *in vivo*. Cy5-labeled siRNA-L_2, siRNA was injected *i.v.* into CD1 mice and blood was collected after 20 minutes. Serum isolated from blood components was evaluated via PAGE gel retardation assay for the presence of Cy5-labeled oligonucleotide. Mice injected with siRNA had no Cy5 signal in the serum, but mice injected with siRNA-L_2 showed faint bands corresponding to the unbound siRNA-L_2 and a stronger band corresponding to albumin-bound siRNA-L_2. C) siRNA and siRNA-L_2 degrade over time in 60% FBS at 37°C. siRNA-L_2 degrades more slowly than siRNA. D) DNA, DNA-L_2 degrade on a similar time scale to siRNA. siRNA-L_2.

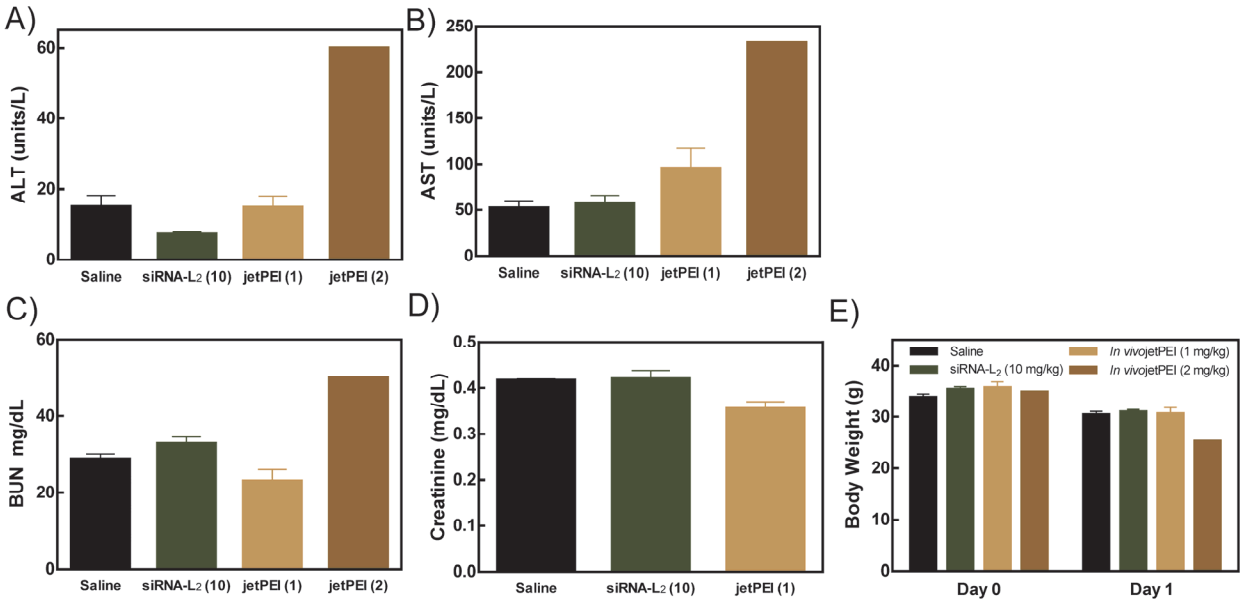

Figure S4. Blood chemistry panel and body weight of mice injected with siRNA-L_2 (10 mg/kg) or *in vivo* jetPEI loaded with siRNA (1 mg/kg, 2 mg/kg). A) ALT: alanine aminotransferase; B) AST: aspartate aminotransferase; C) BUN: blood urea nitrogen; D) Creatinine, (reading for *in vivo* jetPEI at 2 mg/kg was not measurable). E) Body weight pre-injection (day 0) and 24 hours post-injection (day 1). n = 4, standard error is plotted. 3 of 4 mice in the 2 mg/kg *in vivo* jetPEI did not survive treatment and could not be included in analysis.

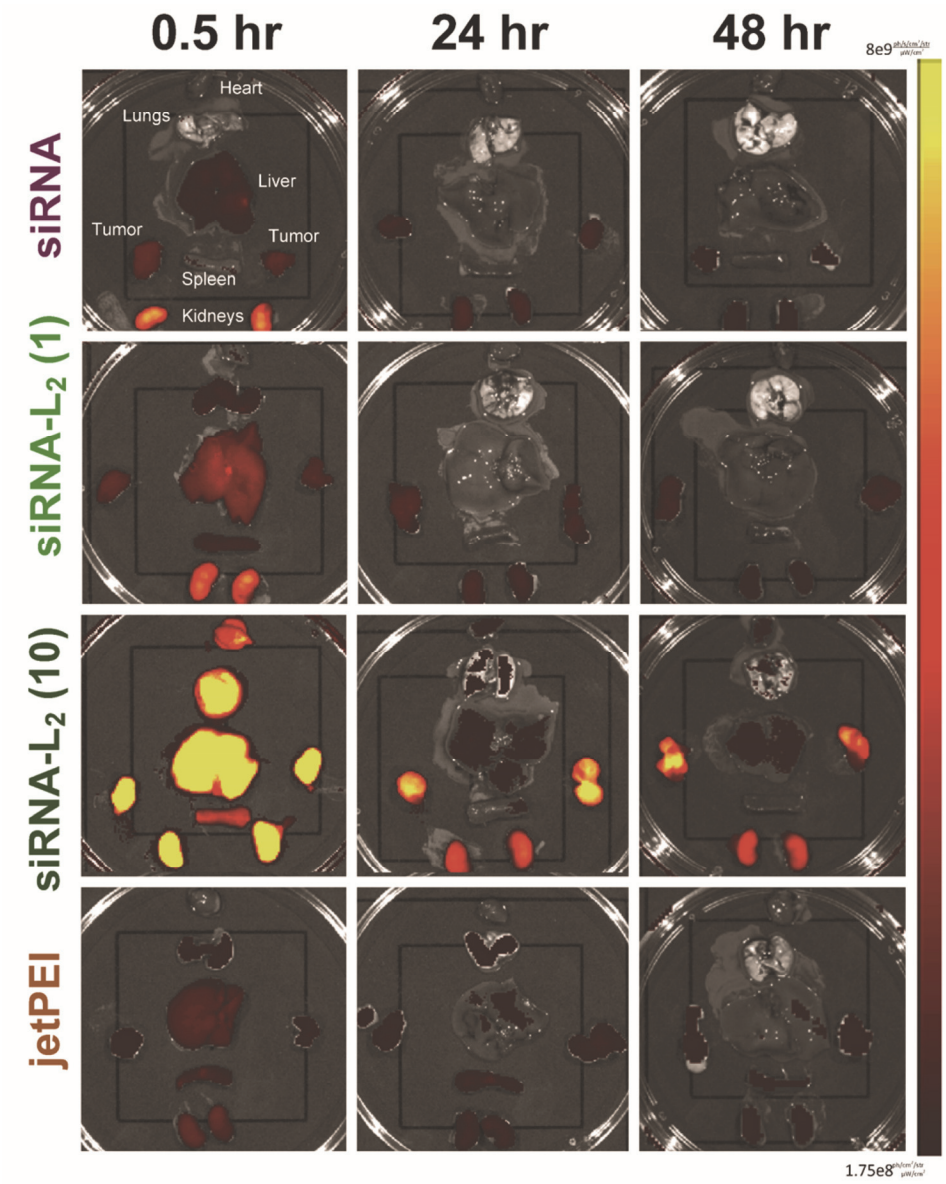

Figure S5. Representative images of biodistribution to the organs in orthotopic tumor-bearing mice. siRNA-L_2 was evaluated at 1, 10 mg/kg and jetPEI NPs were evaluated at 1 mg/kg.

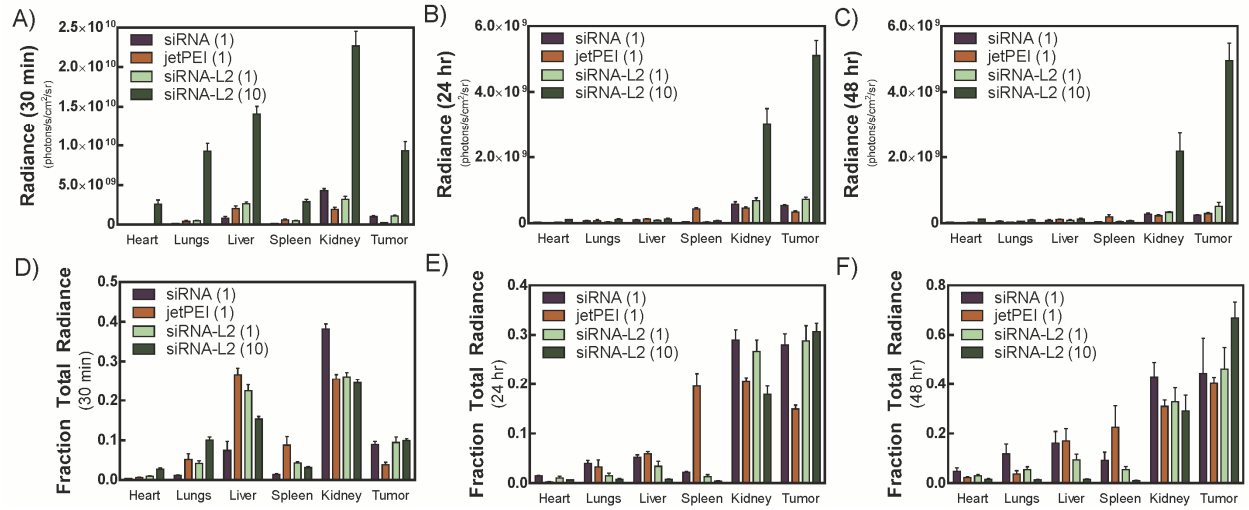

Figure S6. In an orthotopic tumor model, absolute radiance per each organ at A) 30 minutes, B) 24 hours, C) 48 hours and fraction of total radiance per each organ at D) 30 minutes, E) 24 hours, F) 48 hours. n = 4, standard error plotted.

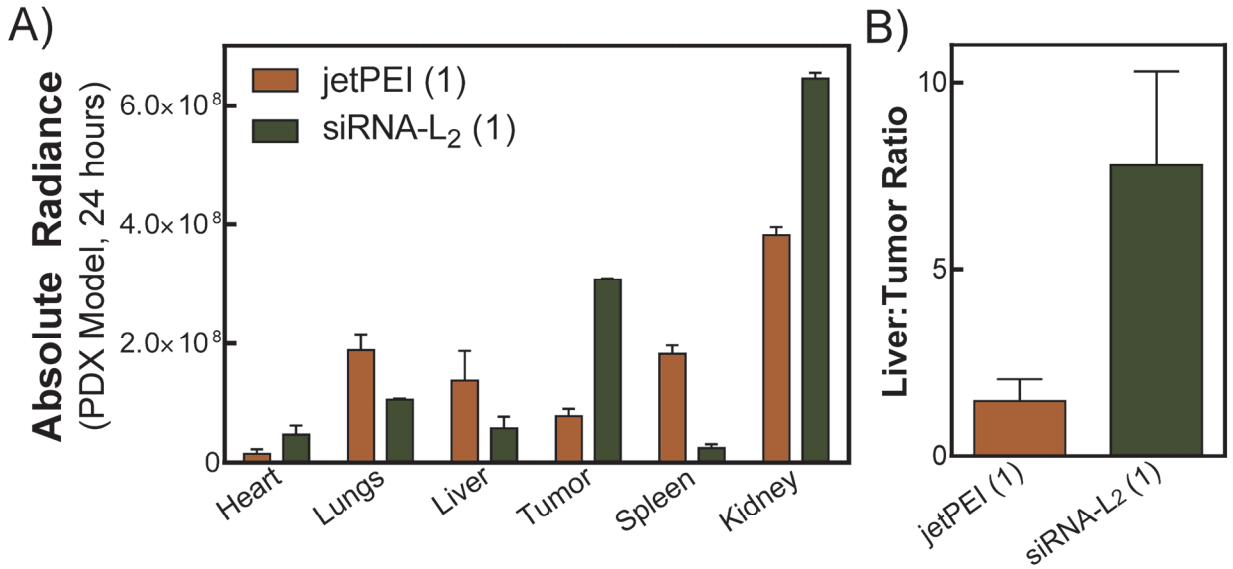

Figure S7. In a PDX tumor model, A) absolute radiance per each organ at 24 hours and B) tumor:liver ratio of jetPEI NPs and siRNA-L_2 in a PDX tumor model after intravenous injection at 1 mg/kg. n = 2, standard error plotted.

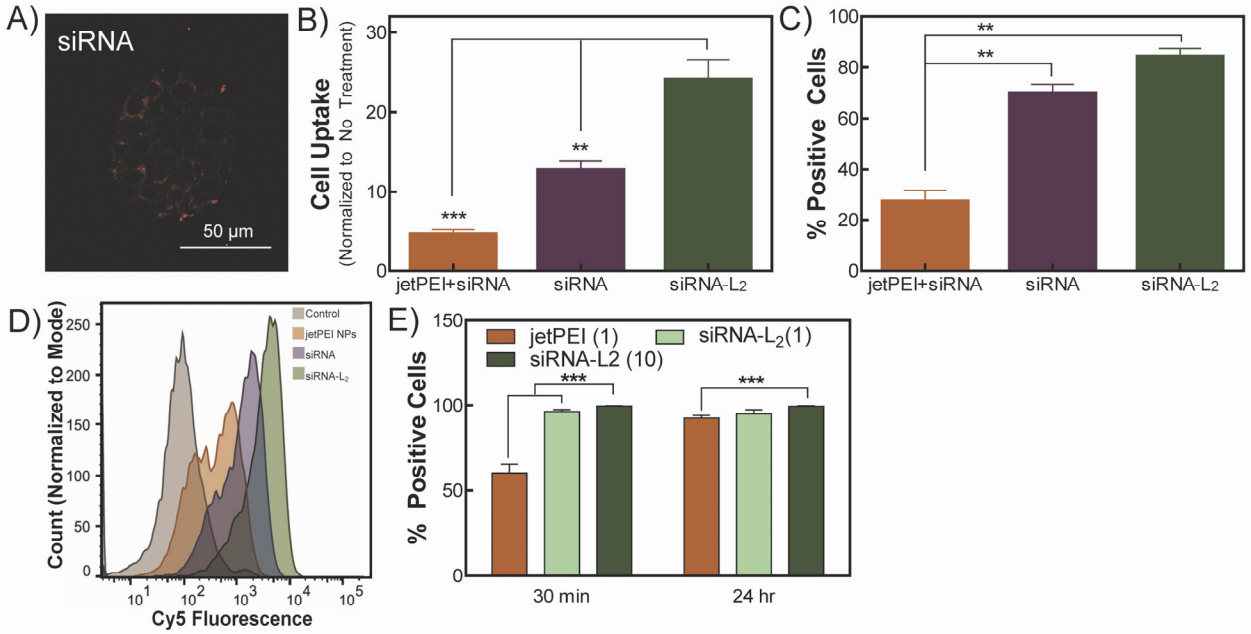

Figure S8. A) Representative image of tumor spheroid uptake for siRNA. B) Cellular uptake, as evaluated by flow cytometry, of MCF-7 breast cancer cells grown in tumor spheroids. Data are expressed as fold increase in fluorescence relative to untreated cells. Treatment with *in vivo* jetPEI complexes resulted in significantly less uptake than siRNA, while siRNA-L_2 achieved the highest uptake. C) Percentage positive cells, as evaluated by flow cytometry, of MCF-7 breast cancer cells grown in tumor spheroids. Treatment with *in vivo* jetPEI complexes resulted in significantly fewer positive cells than siRNA and siRNA-L_2, consistent with its poor penetration into the interior of the tumor spheroids. D) Representative histograms of flow cytometric evaluation of Cy5-labeled siRNA uptake by MCF-7 breast cancer cells grown in tumor spheroids. E) Percentage cy5 siRNA positive tumor cells isolated from orthotopic xenograft mouse tumors. n = 6 to 8. n = 3, standard error plotted; ** = $p<0.01$, ***=$p<0.001$.

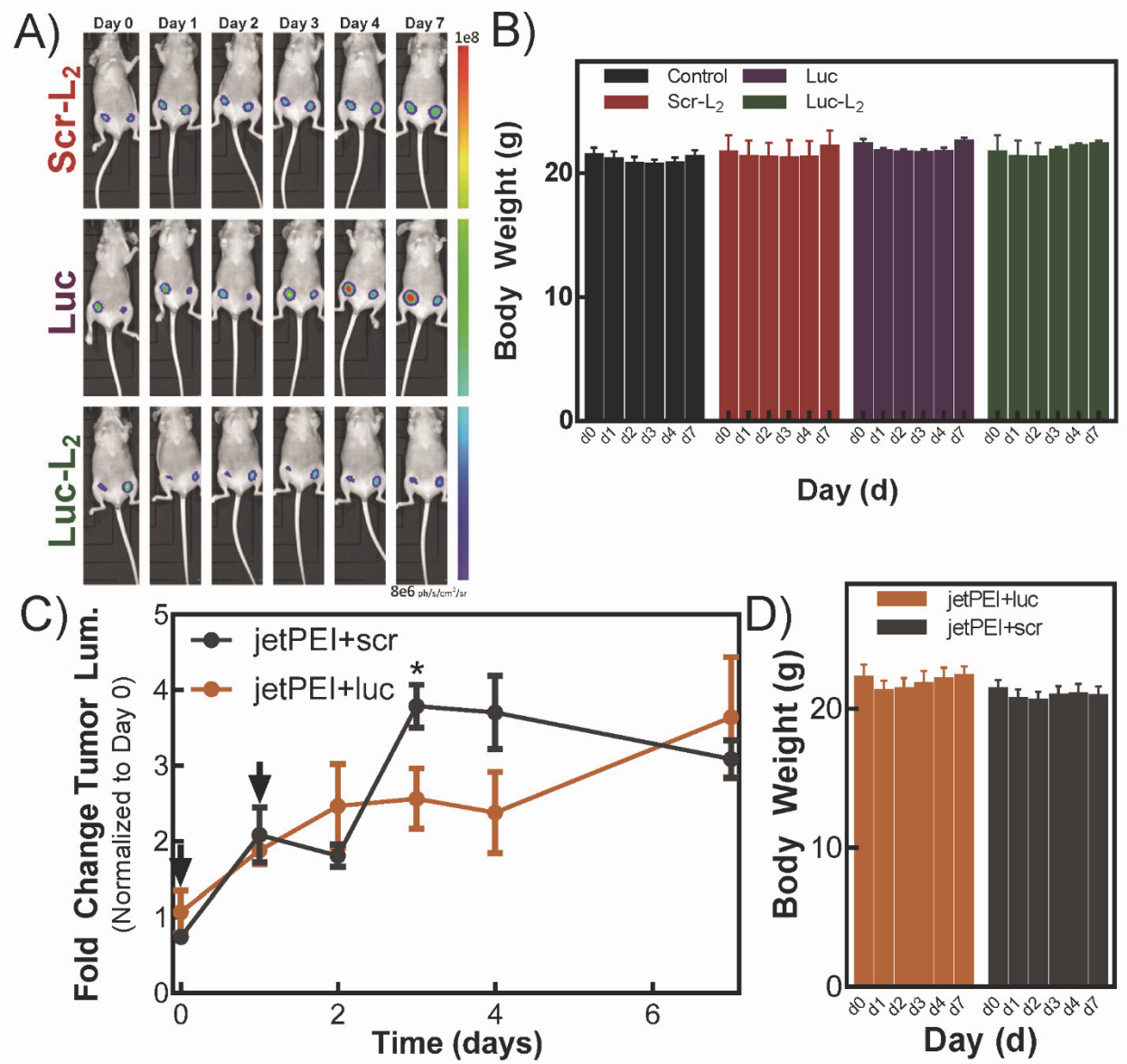

Figure S9. A) Representative images of tumor luminescence in mice with orthotopic luciferase-expressing tumors, treated with luc-L_2, luc, or scr-L_2 at 10 mg/kg on day 0 and 1. B) Mouse body weight after treatment with luc-L_2, luc, or scr-L_2 at 10 mg/kg on day 0 and 1; body weight is consistent across treatment groups over the course of the experiment. n = 5. C) Gene silencing jetPEI NPs complexed with luc compared to scr siRNA in an orthotopic xenograft mouse tumor model; treatment at day 0 and 1 (as indicated by arrows) at 1 mg/kg, n of 8; * = $p < 0.05$. D) Mouse body weight after treatment jetPEI NPs complexed with luc or scr siRNA at 1 mg/kg on day 0 and 1; body weight is consistent across treatment groups over the course of the experiment. n = 5. Standard error is plotted for all.

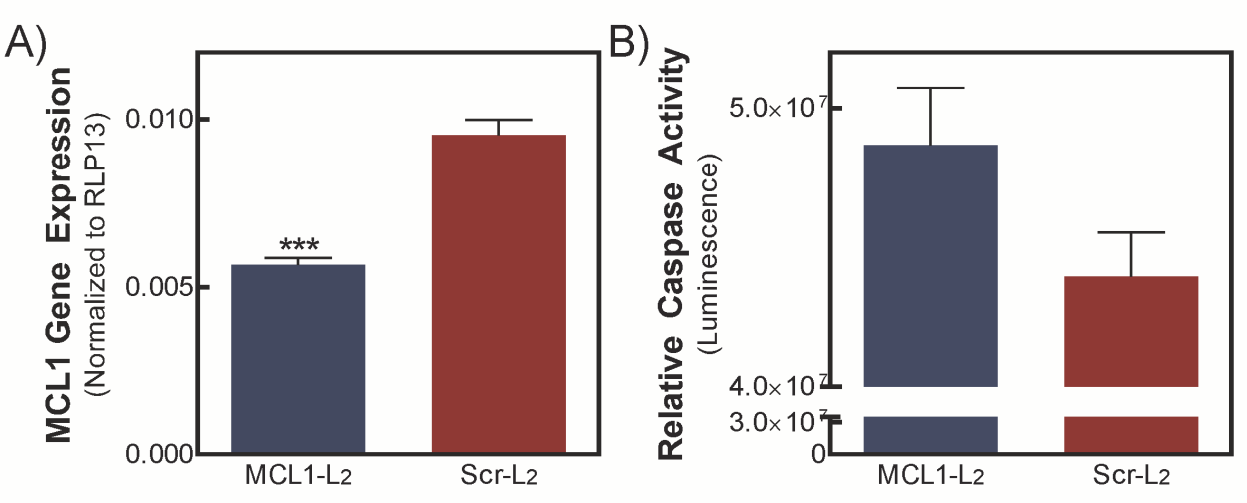

Figure S10. **Figure 6.** siRNA-L_2 A) silences therapeutic gene MCL-1 and B) increases caspase activity *in vitro*. Treatment of MCF-7 cells at 200 nM for 24 hours in 10% serum; n = 3, standard error plotted. *** $p < 0.01$.